J. Membrane Biol. 109, 269–281 (1989)

The Journal of
Membrane Biology
© Springer-Verlag New York Inc. 1989

Analysis of the Blocking Activity of Charybdotoxin Homologs and Iodinated Derivatives Against Ca^{2+}-Activated K^+ Channels

Kathryn Lucchesi, Arippa Ravindran, Howard Young, and Edward Moczydlowski
Department of Pharmacology and Department of Cellular and Molecular Physiology, Yale University School of Medicine, New Haven, Connecticut 06510

Summary. Two charybdotoxin peptides were purified from venom of the Israeli scorpion, *Leiurus quinquestriatus hebraeus*. Microsequencing of the most abundant toxin, ChTX-Lq1, revealed identity with the 37-residue peptide previously sequenced by Gimenez-Gallego et al. [Gimenez-Gallego, G., et al., *Proc. Natl. Acad. Sci. USA* **85**:3329–3333 (1988)]. Sequence data on the minor peptide, ChTX-Lq2, showed substantial homology to ChTX-Lq1 with differences observed at eight positions. These two charybdotoxin sequences, along with that of noxiustoxin, define a distinct family of scorpion peptide toxins with activity against K^+ channels. Both charybdotoxin homologs inhibited Ca^{2+}-dependent K^+ efflux from human erythrocytes with similar potency, $K_{0.5} \simeq 40$ nM. In planar bilayer assays of single K(Ca) channels from rat muscle, ChTX-Lq1 and ChTX-Lq2 blocked with intrinsic K_d's of 1.3 and 43 nM, respectively, in the presence of 50 mM external KCl. A new application of dwell-time histogram analysis of single-channel blocking events was used to characterize the kinetic homogeneity of toxin samples and the blocking kinetics of ChTX derivatives. The lower blocking affinity of ChTX-Lq2 was the combined result of a faster dissociation rate and a slower association rate as compared to ChTX-Lq1. The blocking activity of two mono-iodinated derivatives of ChTX-Lq1 was also analyzed. Blocked dwell-time histograms of the iodinated peptides were characterized by predominately brief (0.2–2 sec) blocking events in comparison to the native toxin (20 sec). Histogram analysis revealed that mono-iodination of ChTX-Lq1 impairs blocking activity by adverse effects on both dissociation and association rate constants. Frequency density histograms of single channel blocking events provide a sensitive assay of toxin purity suitable for quantitating structure-activity relationships of charybdotoxin derivatives.

Key Words charybdotoxin · erythrocytes · iodination · kinetics · peptides · potassium channels · scorpions

Introduction

Ion channels responsible for potassium-selective conductances of cell membranes are noted for their functional diversity and susceptibility to modulation. Given their important role, potassium channels involved in regulating the electrical status of cell membranes could be effective targets of pharmacological intervention; and, indeed, several types of drugs that appear to act on potassium channels have been described [11]. In addition to synthetic compounds, venoms of bees, scorpions and snakes are sources of peptide toxins such as apamin, noxiustoxin, charybdotoxin and dendrotoxin that specifically inhibit potassium channel activity in electrophysiological assays (for review *see* Ref. 21). These toxins are valuable as natural ligands for discriminating classes of potassium channels and as probes in the development of potassium channel biochemistry. One of these toxins, charybdotoxin, was originally identified by its potent blocking activity against a large conductance calcium-activated potassium channel [18], but has since been demonstrated to be a high-affinity blocker of certain voltage-dependent potassium channels in thymocytes [6, 14] and voltage-dependent potassium channels cloned from *Drosophila* and expressed in frog oocytes [17]. In view of this unique blocking activity against a subset of voltage-sensitive potassium channels with diverse gating behaviors, appropriate charybdotoxin derivatives or homologs could be used to investigate the distribution of potassium channel subtypes in various tissues.

Toward this goal, we describe the purification and sequencing of two homologous charybdotoxin peptides from venom of the Israeli scorpion, *Leiurus quinquestriatus hebraeus*. Our sequence data reinforces previous evidence [12, 24] suggesting that charybdotoxins represent a new family of scorpion peptide toxins distinct from sodium channel toxins that are present in the same venom. We find that the charybdotoxin peptides, ChTX-Lq1 and ChTX-Lq2, inhibit Ca^{2+}-activated K^+ efflux from human erythrocytes with equal potency but exhibit a 30-fold difference in relative affinity for

blocking K(Ca) channels of rat skeletal muscle. The single-channel assay of rat muscle K(Ca) channels in planar bilayers is used to assess the effect of iodination on charybdotoxin blocking activity. A new application of histogram analysis is also presented for analyzing the blocking kinetics of low-affinity toxin derivatives. This method can be used in cases where toxin samples are unavoidably contaminated with small amounts of a high-affinity congener that is difficult to chemically separate. Our results indicate that iodination reduces charybdotoxin blocking activity by both decreasing the association rate and increasing the dissociation rate of toxin binding. Part of this work was presented in abstract form at the 1989 meeting of the Biophysical Society [15].

Materials and Methods

Purification of Charybdotoxin Peptides

Lyophilized venom of *Leiurus quinquestriatus hebraeus* was purchased from Latoxan (Rosans, France). Two hundred mg venom was suspended in 25 ml of 10 mM NH_4 OAc,* pH 7, vortexed and centrifuged at 25,000 × *g* for 15 min. The insoluble mucous pellet was similarly extracted three times and the combined 100-ml supernatant was fractionated on an 80-ml column of Biorex-70 (200–400 mesh) cation exchange resin (Biorad, Richmond, CA), previously equilibrated with 10 mM NH_4 OAc, pH 7.0. After loading the sample, the column was eluted at 0.5 ml/min with 50 ml of 10 mM NH_4 OAc followed by a linear gradient of 300 ml 10 mM NH_4 OAc/300 ml 800 mM NH_4 OAc at pH 7. A typical absorbance (280 nm) and conductivity profile of 5-ml fractions is shown in Fig. 1, top panel.

The most basic peak (peak *G*) eluting at 0.47–0.52 M NH_4 OAc was lyophilized to dryness and redissolved in 1 ml 0.05% TFA. Aliquots (0.1 ml) of this sample were fractionated by reverse phase HPLC on a C-18 Vydac column (0.46 × 25 cm, 5 μm, Nest Group, Southboro, MA) using a 30-min linear gradient of 100% A to 100% B at 1 ml/min (A = 0.05% TFA; B = 0.045% TFA, 70% vol/vol CH_3CN). An elution profile monitored at 220 nm is shown in the bottom panel of Fig. 1. The major peak of ChTX activity eluting near 13 min (Lq1) and a smaller trailing peak (Lq2) were pooled and separated on the same column using a longer and shallower gradient: 5 min buffer A followed by a 40 min linear gradient of 100% A to 60% A/40% B. In this separation, Lq1 and Lq2 exhibited retention times of 33.1 ± 0.3 min (SD, $n = 3$) and 33.9 ± 0.2 min ($n = 8$), respectively. Figure 2 shows expanded portions of chromatograms of >95% pure Lq1 and Lq2 obtained using the 40-min gradient. Absolute concentrations of purified Lq1 and Lq2 used in subsequent experiments were based on quantitative amino acid analysis. Purified ChTX peptides bind strongly to glass at low ionic strength. Rinsing glassware with a solution of 0.05% TFA and 35% CH_3CN during transfer procedures resulted in improved yields.

* *Abbreviations:* ChTX, charybdotoxin; K(Ca) channel, Ca^{2+}-activated K^+ channel; Mops, 3-(N-morpholino)propanesulfonic acid; NH_4OAc, ammonium acetate; TFA, trifluoroacetic acid.

Amino Acid Analysis and Sequencing

The composition of peptide samples was determined with a Beckman 121M amino acid analyzer using ninhydrin detection after vacuum hydrolysis in 6 N HCl at 110°C for 24 hr. Cysteine was similarly determined after performic acid oxidation. Charybdotoxins Lq1 and Lq2 were reduced in the presence of 4 mM dithiothreitol, 0.1 M ammonium bicarbonate, pH 8 (1 hr, 50°C) and alkylated with 8.3 mM iodoacetamide (1 hr, 22°C). Alkylated peptides were repurified by reverse phase HPLC and sequenced using an Applied Biosystems 470A gas phase sequenator with on line HPLC detection of phenylthiohydantoin amino acid derivatives. Low first cycle yields with both Lq1 and Lq2 indicated that these peptides lack a free amino terminus. As reported for the ChTX peptide isolated by Gimenez-Gallego et al. [12], we found that Lq1 and Lq2 could be deblocked by treatment with pyroglutamate aminopeptidase [EC 3.4.19.3] (Boehringer Mannheim, Indianapolis, IN). The deblocking reaction was carried out on reduced and alkylated ChTX for 12 hr in the presence of 10 μg/ml enzyme at 22°C following the method of Podell and Abraham [23]. The deblocked peptides were isolated by reverse phase HPLC and sequenced. Unambiguous identification of the first 21 residues was achieved for both Lq1 and Lq2. Portions of the carboxy termini were obtained by sequencing fragments generated by treatment with cyanogen bromide, chymotrypsin [EC 3.4.21.1] or endoproteinase Lys-C [EC 3.4.99.30] using methods adapted from Allen [2].

Iodination of Charybdotoxin Peptides

Iodination of ChTX-Lq1 was performed by the Iodogen (Pierce, Rockford, IL) method or the lactoperoxidase [EC 1.11.1.7]/glucose oxidase [EC 1.1.3.4] method using Enzymobeads (Biorad). Higher yields of active ^{125}I-Lq1a (Fig. 8) were obtained with Enzymobeads. ChTX-Lq1 was radioiodinated both at low specific activity (0.03 Ci/mmol) for bilayer assay of products or at high specific activity (300 Ci/mmol) for binding experiments. Six nmol of lyophilized ChTX-Lq1 was dissolved in 50 μl of 100 mM potassium phosphate, pH 5.5, and the following substrates were added in minimal volumes: 1.4 mM β-D-glucose, 8 nmol NaI and 1.6 nmol $Na^{125}I$ (3 mCi or 0.3 μCi $Na^{125}I$). A suspension of Enzymobeads was prepared by addition of 200 μl 100 mM potassium phosphate, pH 5.5, to a single-use vial of Enzymobeads from the manufacturer. Iodination was initiated by addition of 25 μl Enzymobead suspension. After 10 min at 0°C, the reaction mixture was applied to a 1 ml C-18 Supelclean column (Supelco, Bellefonte, PA) pre-equilibrated with 0.05% TFA. Under these conditions, the ChTX peptides were bound to the column and free ^{125}I was removed by washing five times with 0.6 ml 0.05% TFA. The peptides were recovered by eluting with 1 ml of 70% CH_3 CN, 0.05% TFA. This sample was lyophilized, redissolved in 0.1 ml phosphate buffer, injected on a Vydac C-18 column and eluted for 5 min with 100% A followed by a linear gradient of 100% A to 60% A/40% B over 80 min (1 ml/min). Fractions (0.2 ml) were collected and assayed for radioactivity using a gamma counter (Fig. 8).

Ca^{2+}-Stimulated K^+ Efflux from Human Erythrocytes

Methods for this assay were adapted from previous studies [5, 8]. Blood was freshly drawn from human volunteers into heparinized syringes. The cells were washed three times along with

removal of the buffy coat by centrifugation at 2000 × *g* with 150 mM KCl, 20 mM Tris-HCl, pH 7.4 at 4°C. The washed erythrocytes were resuspended in the same medium at 50% hematocrit and stored at 4°C for up to three days. For K^+ efflux measurements an aliquot of stored cells was washed three times in low K^+ buffer (in mM: 145 NaCl, 0.1 KCl, 1 $MgCl_2$, 1 $CaCl_2$, 5 inosine, 10 Tris-HCl, pH 7.4) and resuspended in this medium at a hematocrit of 2%. K^+ efflux from this cell suspension was monitored at 22°C with a K^+ electrode (Corning, Medfield, MA) and a Corning 150 pH meter in the absolute mV mode. After several minutes of equilibration with constant stirring, 10 μM A23187 (Calbiochem) was added to initiate Ca^{2+}-dependent K^+ flux. K^+ loss was expressed as a percentage of cell K^+ content determined by adding 20 μM digitonin at the end of each experiment. The inhibitory effect of ChTX was measured relative to paired controls in the absence of ChTX using a 5-min time point after the addition of A23187.

Planar Bilayer Assay of ChTX Blocking Activity

Methods for incorporating and recording current fluctuations of single K(Ca) channels have been detailed previously [4, 18]. Bilayers were formed from a solution of 20 mg/ml bovine brain phosphatidylethanolamine and 5 mg/ml diphytanoylcholine (Avanti, Birmingham, AL) in decane. The "internal" chamber (0.6 ml) contained 10 mM Mops-KOH, pH 7.4, 100 mM KCl and 50 to 100 μM $CaCl_2$. The "external" chamber (1.2 ml) contained 10 mM Mops-KOH, pH 7.4, 50 mM KCl and 0.1 mM EDTA. Incorporation of K(Ca) channels was observed after addition of 1 to 5 μg/ml rat muscle plasma membrane vesicles to the internal side. Because of the strict Ca^{2+} requirement for channel activation, these conditions insure that the external side corresponds to the side of an incorporated channel that is extracellular in vivo. Bilayers containing a single K(Ca) channel were typically stable for 1 hr. Toxins were added to the external side with constant stirring, and blocking events were recorded on chart paper with an analog recorder (General Scanning, Watertown, MA) at 5 mm/sec. Measurements of dwell times of blocked and unblocked events accurate to 0.1 sec were taken from the chart record with the aid of a TG1017 digitizing tablet (Houston Instruments, Austin, TX). Histogram displays of event populations and fits to exponential distributions were performed according to the method of Sigworth and Sine [27]. Dr. Steven Sine graciously supplied the programs PCHST, PCDIS and PCFIT for use on an Indec Systems LSI-1173 computer (Sunnyvale, CA).

Results

Isolation and Structure of Charybdotoxins Lq1 and Lq2

Purification of ChTX blocking activity from *L. quinquestriatus* venom has been described previously by two other laboratories [12, 28]. These studies showed that fractionation of crude scorpion venom on various cation exchange resins by conventional low pressure chromatography followed by reverse phase HPLC is an efficient scheme for peptide toxin purification. The original purification of Smith et al. [28] yielded apparently pure toxin by criteria of

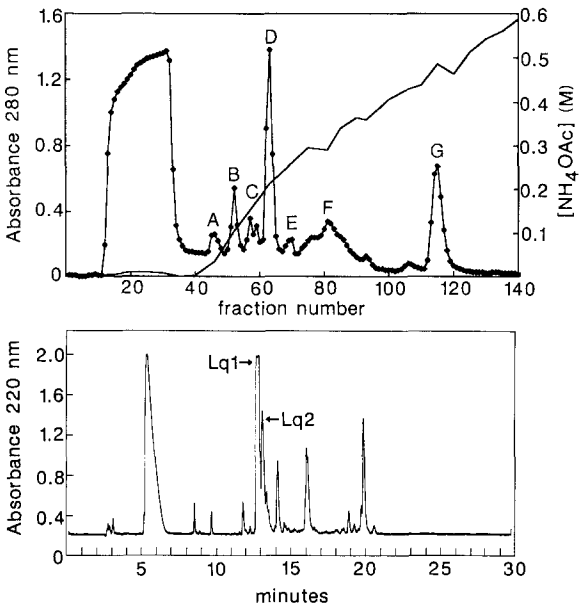

Fig. 1. Purification of charybdotoxins Lq1 and Lq2 from *Leiurus quinquestriatus* venom. Top panel: cation exchange chromatography of 200 mg lyophilized scorpion venom on Biorex-70 resin. Bottom panel: reverse phase HPLC of peak *G* from top panel. Peak *G* was lyophilized to dryness and redissolved in 0.05% TFA. An aliquot (0.1 ml) of this sample was chromatographed on a C-18 Vydac column with a linear gradient of 0–70% CH_3CN in 0.05% TFA over 30 min at a flow rate of 1 ml/min

HPLC and gel electrophoresis, but discrepancies in molecular weight as estimated by amino acid composition *vs.* gel electrophoresis suggested the presence of impurities. Subsequently, Gimenez-Gallego et al. [12] isolated a peptide of 37 residues with a blocked amino terminus that was sequenced by Edman degradation after treatment with pyroglutamate aminopeptidase. Proceeding along similar lines, we purified two forms of ChTX activity with different blocking kinetics.

Figure 1 (top panel) shows a typical fractionation profile of crude *Leiurus* venom on Biorex-70 cation exchange resin. After an initial void peak that elutes at low ionic strength, six major peaks marked *A–F* typically elute in the range of 0.05 to 0.4 M NH_4 OAc. *Leiurus* venom is an established source of peptide toxins that modify gating kinetics of voltage-dependent sodium channels [9]. To assay for the presence of Na-channel toxins, lyophilized peaks of Fig. 1 (top) were tested for stimulation of binding of ^{3}H-batrachotoxinin A 20-α-benzoate to rat brain membranes using a published method [10]. Peaks *A–F* were found to stimulate ^{3}H-batrachotoxin binding from two- to sixfold, while peak *G* exhibited no effect in this assay (*data not shown*). This implies that peak *G* does not contain sodium channel toxins. Planar bilayer assays of K(Ca)

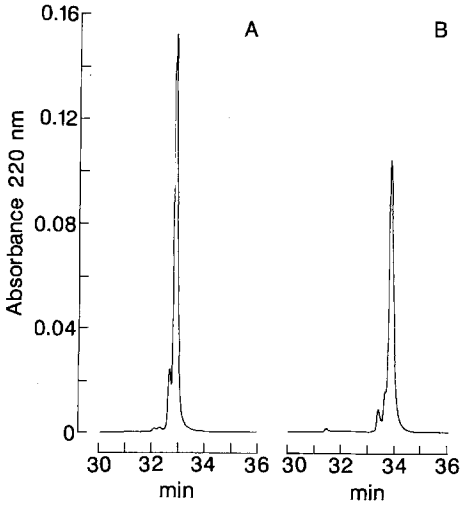

Fig. 2. Reverse phase HPLC analysis of purified charybdotoxin preparations. (*A*) ChTX-Lq1. (*B*) ChTX-Lq2. Expanded segments of 45-min chromatograms of approximately 1 nmol of the purified peptides are shown. Other details are given in Materials and Methods

channels from rat muscle indicated that peak *G* was the only peak containing K-channel blocking activity. This peak was therefore used as a source of ChTX activity for further purification.

Reverse phase HPLC separation of peak *G* on a Vydac C-18 column is shown in the bottom panel of Fig. 1. ChTX activity elutes in a major (Lq1) and minor (Lq2) peak near 13 min in this particular system. Additional repetitive separation using a long and shallow CH_3CN gradient was necessary to resolve these peaks (Fig. 2*A* and *B*). As discussed later, purification of ChTX-Lq2 from ChTX-Lq1 could be monitored by shorter blocked times of Lq2 *vs.* Lq1 in the bilayer assay. Final preparations of ChTX-Lq1 and ChTX-Lq2 were at least 95% homogeneous by HPLC. Pure preparations of ChTX-Lq1 showed a small leading shoulder that we attribute to an inactive oxidation product. Our best ChTX-Lq2 preparation also appeared to contain about 5% of a small peak that runs close to ChTX-Lq1.

Both ChTX-Lq1 and ChTX-Lq2 have blocked amino termini as indicated by insignificant yields (<5%) after gas phase sequencing of the alkylated peptides. Treatment of alkylated ChTX-Lq1 with pyroglutamate aminopeptidase followed by automated sequencing resulted in 21 identifiable cycles of Edman degradation with a sequence identical to that reported by Gimenez-Gallego et al. [12] in these positions. Residues 22–37 of ChTX-Lq1 were also confirmed by overlapping fragments obtained by cyanogen bromide cleavage at met-29 and chymotrypsin cleavage at his-21 and met-29. The amino acid composition of ChTX-Lq1 (Table 1) is also in good agreement with the Gimenez-Gallego sequence of ChTX.

Table 1. Amino acid composition of charybdotoxins Lq1 and Lq2[a]

Amino acid	ChTX-Lq1	ChTX-Lq2
ala	0.2 ± 0.1(0)	0.9 ± 0.1(1)
arg	3.1 ± 0.3(3)	2.4 ± 0.2(3)
asx[b]	3.1 ± 0.2(3)	3.1 ± 0.1(4)
cys	4.9 ± 0.3(6)	ND[d] (6)
glx[c]	3.1 ± 0.3(3)	2.6 ± 0.2(4)
gly	1.4 ± 0.1(1)	2.4 ± 0.4(1)
his	1.3 ± 0.3(1)	1.6 ± 0.6(1)
ile	0.2 ± 0.2(0)	1.1 ± 0.1(1)
leu	1.1 ± 0.1(1)	0.8 ± 0.1(1)
lys	3.9 ± 0.7(4)	3.6 ± 0.3(4)
met	0.8 ± 0.1(1)	1.0 ± 0.1(1)
phe	1.0 ± 0.1(1)	1.0 ± 0.1(1)
pro	0.2 ± 0.1(0)	ND[d] (0)
ser	4.0 ± 0.3(5)	2.9 ± 0.6(4)
thr	3.5 ± 0.3(4)	2.4 ± 0.2(3)
trp	ND[d] (1)	ND[d] (1)
tyr	0.9 ± 0.1(1)	0.6 ± 0.1(1)
val	2.0 ± 0.2(2)	1.0 ± 0.1(0)

[a] Compositions are integer values normalized to the mean of [leu + phe + tyr + 0.5 val] for Lq1 and [ala + phe + ile] for Lq2. Observed values represent the mean ± SD of 11 determinations for Lq1 and of five determinations for Lq2. Integers in parenthesis are expected values based on the proposed sequences of Fig. 3.

[b] asp + asn.

[c] glu + gln + pyroglutamate.

[d] Not determined.

Following a similar approach, sequencing of ChTX-Lq2 yielded three fragments of a closely related peptide. Alignment of these partial sequences leads to a proposed structure of ChTX-Lq2 shown in Fig. 3. The observed amino acid composition of ChTX-Lq2 (Table 1) contains a few discrepancies with this proposed sequence. The low values of ser and thr can be rationalized by known destruction of these residues during acid hydrolysis. However, gly and val are about one residue too high and asx and glx are about one residue too low. Such discrepancies could be due to a few sequencing errors or impurities in the ChTX-Lq2 sample. Based on the available sequence data, ChTX-Lq2 differs from ChTX-Lq1 by 8/37 residues, and four of these differences involve conservative substitutions. The close structural homology and identical net charge of ChTX-Lq1 and ChTX-Lq2 account for their similar behavior in ion exchange and reverse phase chromatography.

In Fig. 3 the confirmed sequence of ChTX-Lq1 and the proposed sequence of Lq2 is aligned with that of noxiustoxin (NTX), the first K^+ channel toxin described from scorpion venom [24]. Al-

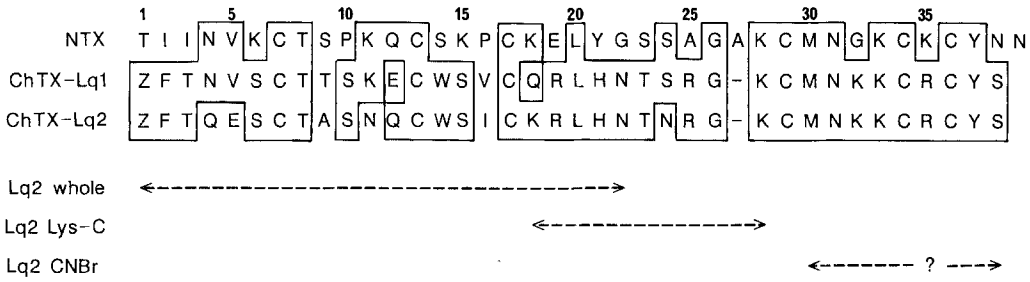

Fig. 3. Comparison of amino acid sequences of noxiustoxin (NTX) with charybdotoxins Lq1 and Lq2. Sequences are aligned for maximum homology by inserting a gap in the Lq1 and Lq2 sequences at position 27 of *NTX*. Identical residues are boxed. The single letter amino acid code is: ala (*A*), arg (*R*), asp (*D*), asn (*N*), cys (*C*), gln (*Q*), glu (*E*), gly (*G*), his (*H*), ile (*I*), leu (*L*), lys (*K*), met (*M*), phe (*F*), pro (*P*), ser (*S*), thr (*T*), trp (*W*), tyr (*Y*), val (*V*), pyroglutamate (*Z*). The bottom map indicates fragments of Lq2 that were sequenced after removal of pyroglutamate (*whole*) and cleavage by endoproteinase *Lys-C* and cyanogen bromide (*CNBr*). For each of the Lq2 fragments the first position is assumed from the known specificity of the cleavage method. The question mark notes a residue that was not identified in the CNBr fragment. The Lq1 sequence is firmly established, while the Lq2 sequence is a proposal based on available data as discussed in the text

though these peptides were separately isolated from Israeli (*Leiurus*) and Mexican (*Centruroides*) species, their close homology indicates that they comprise a family of scorpion toxin peptides distinct from the sodium channel α-toxins and β-toxins. In contrast to the sodium channel toxins, which contain 60–70 residues, 8 cysteines and lack methionine [30], the potassium channel toxins contain 37–39 residues, 6 cysteines and 1 conserved methionine. NTX was originally identified as an inhibitor of squid axon potassium current [7] and has also been found [29] to have low affinity ($K_i \simeq 500$ nM) blocking activity against the rat muscle K(Ca) channel studied here.

Inhibition of Ca^{2+}-Activated K^+ Efflux from Human Erythrocytes

Several laboratories have previously reported that *L. quinquestriatus* venom and ChTX preparations inhibit a Ca^{2+}-activated K^+ efflux from human erythrocytes that is also known as the Gardos effect [1, 8, 31]. The data of Fig. 4 shows that purified ChTX-Lq1 and ChTX-Lq2 are potent inhibitors of K^+ efflux from human erythrocytes induced by the addition of the Ca^{2+} ionophore, A23187. Both toxin homologs inhibited over a similar concentration range and their relative potencies were indistinguishable within the scatter of the data. Fitting of the combined ChTX-Lq1 and ChTX-Lq2 titration data to a Hill equation for the dose dependence of inhibition gave values of $K_{0.5} = 43$ nM and $n = 0.68$, where $K_{0.5}$ is the toxin concentration at 50% inhibition and n is a pseudo-Hill coefficient. A similar value for n was also observed by Castle and Strong [8] using a less pure preparation of ChTX. Since this assay is performed under nonequilibrium conditions, $K_{0.5}$ in this assay may not be equivalent to the

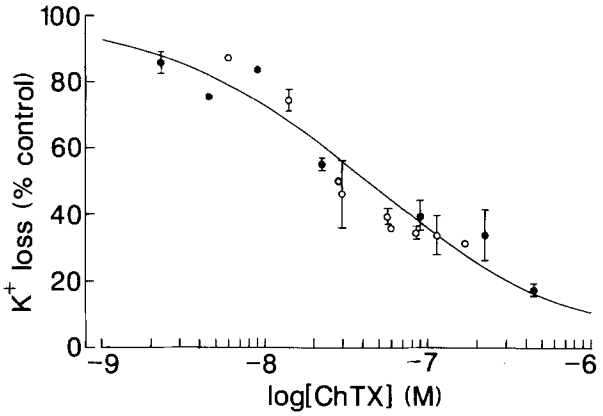

Fig. 4. Inhibition of Ca^{2+}-dependent K^+ efflux from human erythrocytes by charybdotoxins Lq1 and Lq2. Observed K^+ loss as a function of Lq1 and Lq2 concentration is expressed as a percentage of the control K^+ efflux in the absence of charybdotoxin. ●, Lq1; ○, Lq2. The combined data for both toxins were fit to $f = K_{0.5}^n/(K_{0.5}^n + [T]^n)$ where f is the fraction of control K^+ loss, $[T]$ is the toxin concentration, n is a pseudo Hill coefficient and $K_{0.5}$ is the toxin concentration at 50% inhibition. The best fit parameters describing the solid line are $n = 0.68$ and $K_{0.5} = 43$ nM

intrinsic binding constant of these toxins for the erythrocyte K(Ca) channel. Recently, Wolff et al. [31] obtained an IC_{50} of 0.8 nM for ChTX inhibition of the initial rate of K^+ efflux from human red cells. Present data thus indicate that ChTX is the most potent known inhibitor of the Gardos channel.

Blocking Kinetics of Single K(Ca) Channels by ChTX

Anderson et al. [4] and MacKinnon and Miller [16] previously showed that the blocking kinetics of ChTX depend on the open state probability of the K(Ca) channel, external ionic strength, internal

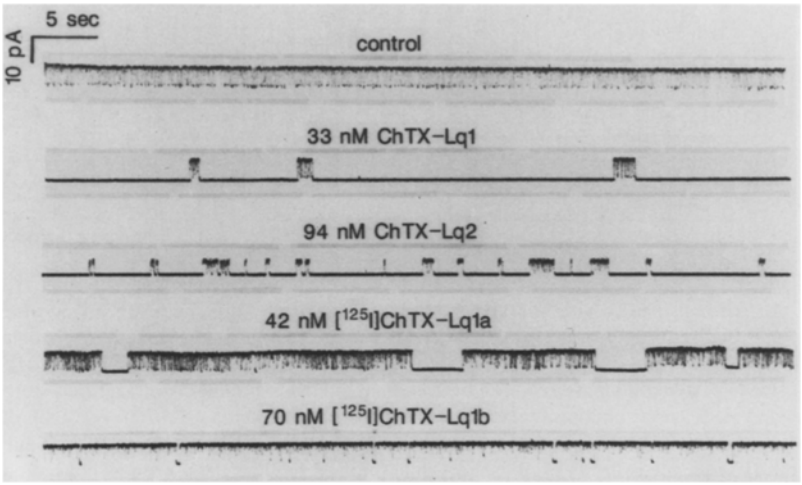

Fig. 5. Block of single K(Ca) channels by charybdotoxins Lq1, Lq2 and two mono-iodinated derivatives of Lq1. Single K(Ca) channels from rat skeletal muscle were incorporated into planar lipid bilayers in the presence of 10 mM Mops-KOH, pH 7.4, with 100 mM KCl, 50 μM $CaCl_2$ (internal solution) or 50 mM KCl, 0.1 mM EDTA (external solution). A control record in the absence of toxins is compared with similar records in the presence of indicated concentrations of various toxin derivatives in the external chamber. Toxin records are shown in the order of decreasing blocking affinity (top to bottom). Holding voltage was +20 mV for all records

concentration of permeant cations and transmembrane voltage. We therefore analyzed toxin blocking kinetics under controlled conditions of +20 mV, 100 mM internal KCl and 50 mM external KCl. The gating of the channel was also "clamped" to an open state probability of 0.8 to 1.0 within unblocked bursts by adjusting internal Ca^{2+} from 50 to 100 μM as necessary to activate a particular channel. For Lq1 and Lq2, the blocking kinetics were also studied at symmetrical 100 and 200 mM KCl to examine the effect of ionic strength.

Figure 5 illustrates the effect of various ChTX peptides on the unitary behavior of K(Ca) channels from rat skeletal muscle incorporated into planar bilayers. As previously shown [4, 16, 18, 28], Lq1 induces the appearance of long-lived blocked events that correspond to residence times of individual toxin molecules on an external binding site. Similar concentrations of Lq2 and iodinated derivatives of Lq1 produced markedly lower blocking probabilities which indicate lower binding affinity. In our preliminary analyses of Lq1 and Lq2 blocking kinetics, it became apparent that the Lq1 behavior was well described by a single-site equilibrium binding reaction as documented previously [4, 16, 18, 28], but that Lq2 and the iodinated derivatives exhibited more complex kinetics. Because this latter behavior depended on the purity of the toxin sample, we realized that the kinetic complexity was due to the inherent difficulty of removing trace amounts of a structurally similar high-affinity toxin from a chemically pure sample of low-affinity toxin. Since further attempts at purification resulted in unavoidable losses of precious peptides of interest, we opted to purify our samples to an acceptable level of chemical purity (90–95%) as determined by HPLC and used the single-channel record as an assay of kinetic homogeneity.

The following scheme was used to analyze toxin blocking kinetics:

$$O \begin{cases} + T_1 \rightleftharpoons OT_1 \\ + T_2 \rightleftharpoons OT_2 \\ \quad \vdots \qquad \vdots \\ + T_n \rightleftharpoons OT_n \end{cases} \tag{1}$$

In this scheme, O refers to an unblocked channel not occupied by toxin; T_1, T_2 . . . T_n refers to a mixture of n toxin derivatives present in equilibrium with a single channel and OT_1, OT_2 . . . OT_n refer to the respective possible blocked states when the channel is occupied by each of the toxins. This scheme is equivalent to a one-site binding reaction with a mixture of n mutually exclusive competitor ligands. In general, each of the toxin derivatives, T_i, can exhibit a unique association rate constant, k_i, a unique dissociation constant, k_{-i}, and an equilibrium constant, $K_i = k_{-i}/k_i$. Since there is a single unoccupied state O, this scheme predicts that the frequency distribution of dwell times in the unblocked state will be a single exponential with a time constant, t_u, equal to the inverse of the sum of all possible toxin association paths leading to a blocked state:

$$t_u^{-1} = \sum_{i=1}^{n} k_i[T_i] \tag{2}$$

where $k_i[T_i]$ is the product of the association rate constant of the ith toxin and its concentration. Because there are n blocked states, each dissociating with a unique k_{-i}, the blocked state distribution is expected to be a sum of exponential components. The cumulative probability form of this distribution is described by the following equations:

$$P(t_b > t) = \sum_{i=1}^{n} f_i \exp(-k_i t) \quad (3)$$

$$f_i = k_i[T_i] \Big/ \sum_{i=1}^{n} k_i[T_i]. \quad (4)$$

Equation 3 states that the probability of a blocked event being longer than time, t, is a sum of n exponentials with the lifetime of each component equal to the reciprocal of the ith toxin dissociation rate, $1/k_{-1}$, and the amplitude of each component, f_i, equal to the association rate leading to the ith blocked state as a fraction of the sum of all the competing association rates (Eq. (4)).

In order to use Scheme 1 for the measurement of single-channel blocking kinetics, one must be able to discriminate toxin-blocking events from normal channel-gating events that are grouped within the unblocked "o" state. In the present application, this is possible because the channel exhibits a high opening probability near 1.0 under the conditions of the assay (+20 mV, 100 μM Ca^{2+}). Under these conditions, residual closing events have a mean lifetime of less than 0.01 sec [20]. By choosing a closed time cutoff of 0.1 sec for the shortest acceptable "blocked" event, we can safely exclude greater than 99% of the gating events from the blocked-time histograms.

In previous studies of the single-channel blocking kinetics of ChTX [4, 16], it was shown that this toxin exhibits mono-exponential histograms for both blocked and unblocked dwell times. In these studies, dwell time histograms were plotted using the cumulative probability representation as shown in Fig. 6 for data obtained with ChTX-Lq1. This graphic representation is visually appealing for single exponential populations of a few hundred events but is unsuitable for fitting multiexponential distributions containing closely spaced time constants or low amplitude components [27]. In the present work, we used cumulative probability histograms to discern whether or not the distributions were mono-exponential and chose a frequency density histogram introduced by Sigworth and Sine [27] to fit and analyze the data. This latter method uses a logarithmic binning of the time axis to enhance detection of multiple components and a square root axis for the ordinate to provide a constant linear standard error from bin to bin.

Figure 7 shows such histograms of blocked and unblocked events accumulated from long single-channel records taken in the presence of ChTX-Lq1 and ChTX-Lq2. Similar histograms for two mono-iodinated derivatives are shown in Fig. 9. In the Sigworth-Sine histogram representation [26], the log-binning procedure results in peaked exponential

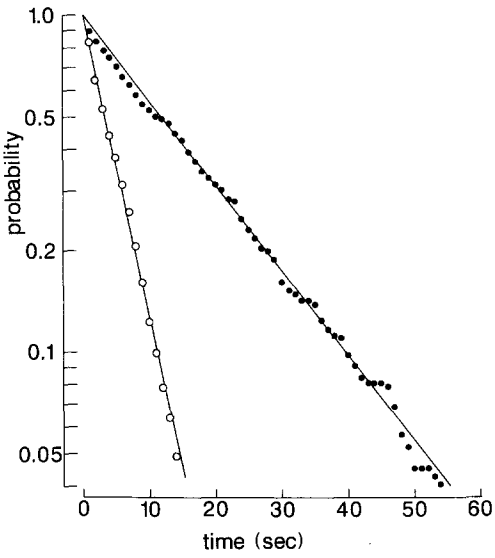

Fig. 6. Cumulative probability histograms of blocked and unblocked events in the presence of ChTX-Lq1. The ordinate is the probability that an event is longer than a time on the abscissa. Blocked and unblocked events were collected from single K(Ca) channels in the presence of 79 nM external ChTX-Lq1. ●, blocked dwell times, n = 419 events, exponential lifetime = 17.2 sec; ○, unblocked dwell times, n = 406 events; exponential lifetime = 4.9 sec

functions with lifetime values occurring at positions of the maxima. In accord with Scheme 1, the histograms of unblocked dwell times are well described by single exponential functions for all the ChTX samples (Fig. 7*B* and *D;* Fig. 9*B* and *D*). Histograms of blocked dwell times could be described by a single exponential function for ChTX-Lq1 (Figs. 6 and 7*A*), but a sum of two exponentials was required to fit the blocked time data for ChTX-Lq2 (Fig. 7*C*).

Since the ChTX-Lq1 data conform to a one-ligand system, the inverse lifetimes of the blocked and unblocked states can be used to directly obtain the association and dissociation rate constants of ChTX-Lq1 from Eqs. (2) and (3), respectively. Derived rate constants for ChTX-Lq1 are summarized in Table 2 for three different ionic conditions. We observed that the association rate constant of Lq1 was strongly dependent on ionic strength, decreasing about 14-fold in the range of 50 to 200 mM external KCl (from 41 to 3 sec^{-1} μM^{-1}). In contrast, the dissociation rate of Lq1 was relatively constant under these conditions (0.047 to 0.062 sec^{-1}). Thus, the observed K_d of Lq1 was higher affinity at low ionic strength and ranged from 1 nM at 50 mM external KCl to 22 nM at 200 mM KCl. The absolute values of the various kinetic parameters (Table 2) are in close agreement with those reported by Anderson et al. [4] for comparable conditions. The

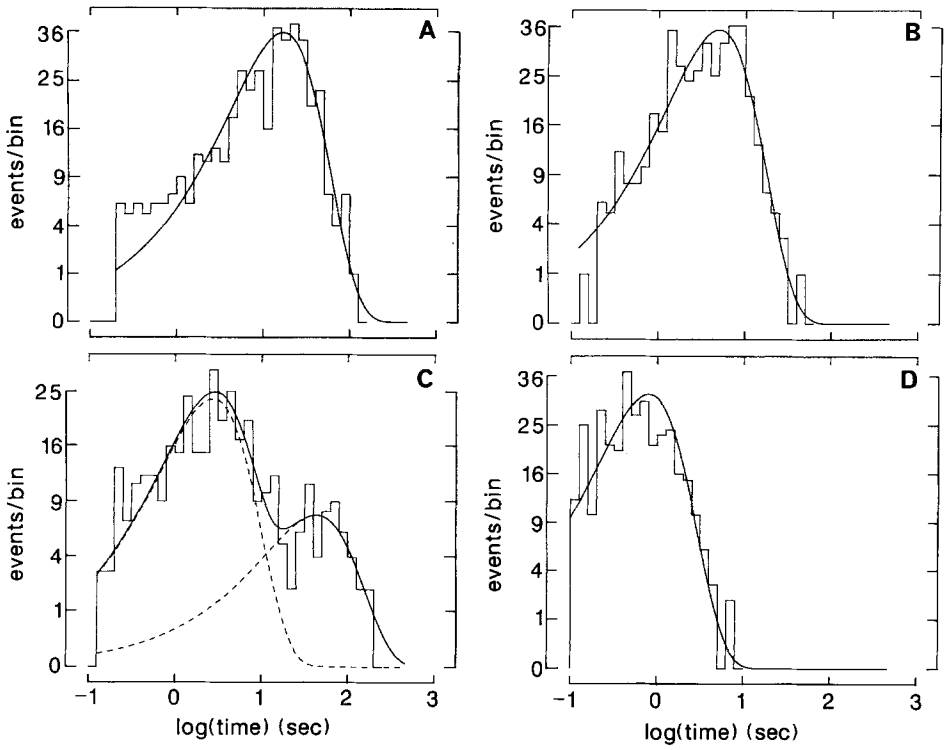

Fig. 7. Histograms and fitted probability density functions of blocked and unblocked events induced by charybdotoxins Lq1 and Lq2. Blocked events were defined as any events in the zero current level longer than 0.1 sec in order to exclude brief channel gating events in the millisecond range. Unblocked events are burst durations in the open state between such blocked events. Histograms are plotted and fitted according to the methods of Sigworth and Sine [27] using a square root scale for the ordinate and a logarithmically binned time axis. (*A*) Blocked events, 79 nM ChTX-Lq1, $n = 419$ events; (*B*) unblocked events, 79 nM ChTX-Lq1, $n = 406$ events; (*C*) blocked, 94 nM ChTX-Lq2, $n = 365$; (*D*) unblocked, 94 nM ChTX-Lq2, $n = 331$. In *A*, *B* and *D* the solid line corresponds to a fit to a single exponential distribution. The respective lifetimes are (*A*) 16.6 sec; (*B*) 4.93 sec; (*D*) 0.80 sec. In *C*, a sum-of-two exponential distribution was used to fit the data, with the dotted line referring to the two individual components and the sum indicated by the solid line. The component lifetimes and respective amplitudes for *C* are: $t_1 = 2.8$ sec, $f_1 = 0.76$; $t_2 = 43$ sec, $f_2 = 0.24$. Conditions: *A* and *B*, 200 mM symmetrical KCl; *C* and *D*, 100 mM internal KCl, 50 mM external KCl

steep dependence of the association rate on external KCl was previously concluded to result from an electrostatic interaction between negative surface charge(s) on the K(Ca) channel and positive surface charge(s) of the highly basic toxin [4]. It is worth noting that the magnitude of this salt dependence is very similar to that observed for the binding of saxitoxin^{2+} to brain and heart sodium channels [25]. Negative surface charge in the vicinity of external toxin binding sites may be a hallmark of voltage-activated channels.

In the case of ChTX-Lq2, the blocked state distribution (Fig. 7*C*) exhibited a major component with a lifetime of $t_1 = 2.8$ sec and amplitude of $f_1 = 0.76$, and a minor component with a lifetime of about $t_2 = 43$ sec and amplitude of $f^2 = 0.24$. Since the prevalence of the short lifetime component directly correlated with the purity of the ChTX-Lq2 sample, this component can be attributed to the actual dissociation rate of ChTX-Lq2. In ten experiments similar to that of Fig. 7*C*, the fitted lifetime value of the longer t_2 component ranged from 13 to 52 sec (mean = 33 ± 14, SD). Since the t_2 lifetime is similar to that observed for pure ChTX-Lq1 (21 ± 5 sec), it is likely that this component corresponds to contaminating Lq1. However, we cannot exclude the possibility that this component is due to another contaminating isotoxin or to a slowly converting conformation of Lq2.

In order to estimate the association rate of Lq2 from the data of Fig. 7*C* and *D*, one can substitute the observed open-state lifetime from Eq. (2) into the denominator of Eq. (4) for a two-component system to obtain:

$$k_1 = f_1/t_u[T_1] \tag{5}$$

where f_1 is the amplitude of the short lifetime component in Fig. 7*C*, t_u is the observed unblocked lifetime from Fig. 7*D* and $[T_1]$ is the estimated concen-

Table 2. Kinetic parameters for block of K(Ca) channels from rat skeletal muscle by charybdotoxins Lq1, Lq2 and two mono-iodinated derivatives of Lq1[a]

Toxin	[KCl] in/out (mM)	k_d (sec^{-1})	k_a ($\times 10^{-6}$ sec^{-1} M^{-1})	K_d (nM)	n
ChTX-Lq1	200/200	0.062 ± 0.004	3.0 ± 0.4	22.5 ± 2.2	9
	100/100	0.052 ± 0.004	9.5 ± 1.7	5.7 ± 0.9	3
	100/50	0.047 ± 0.006	41 ± 10	1.3 ± 0.3	4
ChTX-Lq2	200/200	0.51 ± 0.02	0.34 ± 0.08	1800 ± 600	3
	100/100	0.34 ± 0.02	1.9 ± 0.1	180 ± 5	5
	100/50	0.36 ± 0.04	10 ± 2	43 ± 5	3
^{125}I-Lq1a	100/50	0.48 ± 0.07	0.90 ± 0.28	860 ± 250	6
^{125}I-Lq1b	100/50	5.1 ± 0.3	0.42 ± 0.18	15000 ± 7000	2

[a] The holding voltage was +20 mV in all experiments. Blocking kinetics were studied for various internal (in) and external (out) KCl concentrations as indicated. Uncertainties refer to the standard error of n determinations or the range for $n < 3$.

tration of ChTX-Lq2 in the assay based on amino acid analysis. Kinetic parameters of ChTX-Lq2 obtained by this method are listed in Table 2. At 50 mM external KCl, the estimated K_d for ChTX-Lq2 is about 30-fold lower affinity than that of ChTX-Lq1 due to the combined effects of an eightfold faster dissociation rate and a fourfold slower association rate. The association rate of ChTX-Lq2 also exhibits a steep dependence on ionic strength as found for ChTX-Lq1. Assuming that the long lifetime component of blocked events in Fig. 7*C* is due to Lq1, we can use the directly measured association rate of pure Lq1 (Table 2) to estimate its concentration in the ChTX-Lq2 sample by the use of a relation analogous to Eq. (5). Such calculations indicate that the level of contamination of ChTX-Lq1 in the ChTX-Lq2 sample is about 8%, in reasonable agreement with the estimate of 5% by HPLC.

Effect of Iodination on Blocking Activity of ChTX-Lq1

Figure 8 shows a reverse phase HPLC separation of reaction products obtained from iodination of 6 nmol ChTX-Lq1 by the lactose peroxidase-glucose oxidase method. The peak corresponding to unreacted ChTX-Lq1 was identified by its characteristic retention time in this particular gradient and by the potent blocking activity of the recovered peak. Comparison of the relative amounts of ^{125}I to peptide, as calibrated by peak area, indicates that peaks *a,b* are mono-^{125}I derivatives and peaks *c,d* are di-^{125}I derivatives. Since there is only one tyrosine residue in Lq1, and tyrosine is more readily iodinated than histidine at pH 5.5 [26], the *a,b* and *c,d* pairs of peaks probably correspond to derivatives that contain monoiodo- and diiodo-tyrosine, respectively.

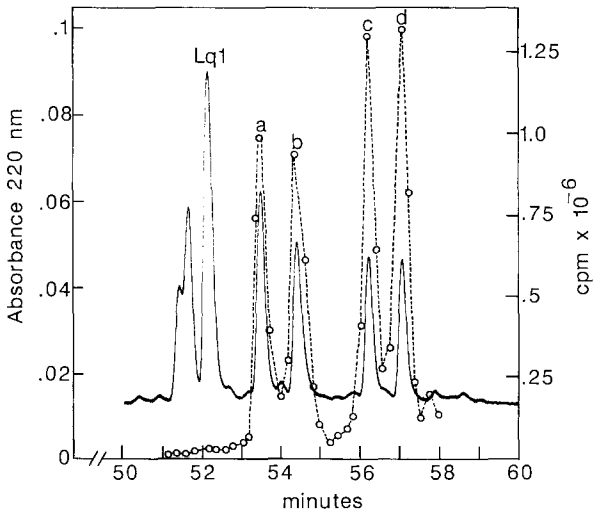

Fig. 8. Reverse phase HPLC separation of radioiodinated derivatives of charybdotoxin Lq1. Six nmol ChTX-Lq1 was iodinated in the presence of 3 mCi Na^{125}I as outlined in Materials and Methods. Unreacted ^{125}I was removed on a 1-ml Supelclean C-18 column. The recovered peptide mixture was injected on a Vydac C-18 column and eluted with a linear gradient of CH_3CN over 80 min. Solid line, chart record of absorbance at 220 nm; dotted line, radioactivity (cpm) in 0.2 ml fractions as measured by a gamma counter. The peak labeled Lq1 was identified as unreacted charybdotoxin. Peaks *a,b* and *c,d* are respectively mono-^{125}I and di-^{125}I derivatives of Lq1. The peak to the immediate left of Lq1 appears to be a nonradioactive oxidation product of Lq1

The curious pattern of doublet peaks can be explained by oxidation of Lq1 that also occurs during the iodination reaction. The unlabeled peak to the immediate left of *Lq1* in Fig. 8 appears to be a noniodinated oxidation product, since this peak is also observed when iodine is left out of the reaction mixture. Since methionine is an easily oxidized residue [26], this unlabeled peak could be due to a

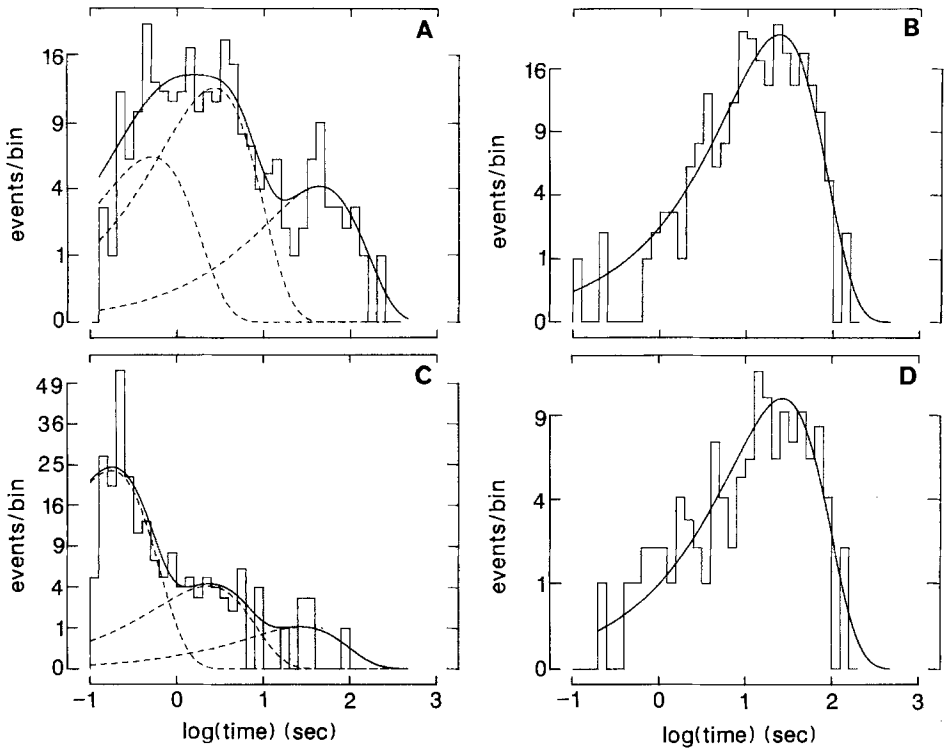

Fig. 9. Histograms and fitted probability density functions of blocked and unblocked events observed in the presence of two mono-iodinated derivatives of ChTX-Lq1. Blocked and unblocked event populations were plotted and analyzed as described in Fig. 5. (*A*) Blocked events, 84 nM ^{125}I-Lq1a, $n = 246$ events; (*B*) unblocked events, 84 nM ^{125}I-Lq1a, $n = 242$ events; (*C*) blocked, 50 nM ^{125}I-Lq1, $n = 217$; (*D*) unblocked, 50 nM ^{125}I-Lq1b, $n = 117$. In *B* and *D* the solid line corresponds to a single exponential distribution with respective lifetime values of (*B*) 23.7 sec; (*D*) 26.9 sec. In *A* and *C*, a sum-of-three exponential distribution was used to fit the data. The component lifetimes and respective amplitudes are: (*A*) $t_1 = 0.51$ sec, $f_1 = 0.27$; $t_2 = 2.7$ sec, $f_2 = 0.55$; $t_3 = 43$ sec. $f_3 = 0.18$. Similarly for *C*: $t_1 = 0.17$ sec, $f_1 = 0.82$, $t_2 = 2.3$ sec, $f_2 = 0.14$, $t_3 = 27$ sec, $f_3 = 0.04$. Conditions: 100 mM internal KCl, 50 mM external KCl

methionine-sulfoxide derivative generated by hydrogen peroxide produced during the reaction. Thus, the closely eluting pairs of iodinated peaks may represent pairs of oxidized and nonoxidized derivatives. A similar HPLC profile of iodinated products was also observed using Iodogen to catalyze the reaction; however, this method gave substantially lower yields of peaks *a* and *c* (*not shown*).

To enhance our ability to detect blocking activity by the iodinated derivatives, bilayer experiments with these derivatives were performed under conditions where native Lq1 exhibits the highest affinity; i.e., 50 mM external KCl. However, even under these conditions, the data of Fig. 5 indicates that the mono-iodinated derivatives of Lq1 exhibit markedly lower blocking activity. Similar tests of the di-iodinated derivatives of Lq1 indicated that they were essentially devoid of blocking activity (*not shown*).

The blocking kinetics of the two mono-iodinated Lq1 derivatives were analyzed by dwell time histograms as described for the Lq2 homolog. Histograms of unblocked events are mono-exponential for ^{125}I-Lq1a and ^{125}I-Lq1b (Fig. 9*B* and *D*), but the blocked-time histograms of these derivatives exhibited multi-exponential distributions with predominantly brief blocking events (Fig. 9*A* and *C*) compared to the native peptide (Fig. 7*A*). Since these derivatives were pooled from closely spaced peaks such as those of Fig. 8, we estimate that the pool of ^{125}I-Lq1a contains about 10% ^{125}I-Lq1b and trace amounts of native Lq1, judging by the relative separation of these fractionated peaks. Likewise, the pool of ^{125}I-Lq1b is estimated to contain about 10% ^{125}I-Lq1a and even lower amounts of native Lq1. This interpretation is consistent with the model of Scheme 1 and the complex three-exponential distribution required to fit the broad time distribution of blocking events observed in Fig. 9*A* and *C*. The theoretical fits to the blocked populations are not very reliable at short times because of the inaccuracy of our measuring technique for dwell times <0.5 sec. Nevertheless, these fits provide valid estimates of the blocking kinetics of the iodinated derivatives. Thus in Fig. 9*A*, the predominant component ($f_2 = 0.55$) with a blocked lifetime of $t_2 = 2.7$

sec is likely to correspond to the dissociation rate of ^{125}I-Lq1a. The second most prevalent component (f_1 0.27) with a lifetime of $t_1 = 0.5$ sec is similar to that observed for the major component of ^{125}I-Lq1b (Fig. 9*C*). The least prevalent component ($f_3 = 0.18$) of long-lived events has a lifetime ($t_3 = 43$ sec) similar to that of native Lq1. Likewise in Fig. 9*C*, the predominant component ($f_1 = 0.82$) with a blocked lifetime of $t_1 = 0.2$ sec can be assigned to ^{125}I-Lq1b itself and the two longer and less prevalent components with lifetimes of $t_2 = 2.3$ sec and $t_3 = 27$ sec can be identified with the characteristic lifetimes of ^{125}I-Lq1a and native Lq1, respectively. These fitting results and relationships similar to Eq. (5) for a three-component system were used to estimate the association rate constants of ^{125}I-Lq1a and ^{125}I-Lq1b. The results listed in Table 2 indicate that the blocking affinity of ^{125}I-Lq1a is about 10^3-fold lower than that of native Lq1. ^{125}I-Lq1b has an even lower affinity, about 10^4-fold lower than Lq1. Thus, iodination severely reduces the blocking affinity of Lq1 for this particular K(Ca) channel as a result of adverse effects on both the association and dissociation rate constants (Table 2).

Discussion

The two ChTX peptides isolated in the course of our work are members of a newly recognized family of K^+ channel toxins in scorpion venom [12, 18, 24]. The absolute conservation of six cysteine residues among known members of this family (Fig. 2) and more random residue variation at other positions is a common theme of other toxin families targeted against ion channel proteins: e.g., Na^+ channel toxins of scorpions [30], K^+ channel dendrotoxins of mamba snakes [13] and three known classes of channel toxins of *Conus* snails [22]. The presence of conserved cysteines and paired disulfide crosslinking in small peptide toxins is thought to provide structural stability that locks such peptides in a smaller number of available conformations to enhance productive binding to the target [22]. Applications of such natural peptides have led to important advances in defining toxin binding sites coupled to agonist binding or channel gating. Their use has also revealed the phenomenon of channel subtype heterogeneity. Our present results on the similar potency of ChTX-Lq1 and ChTX-Lq2 in the erythrocyte K^+ flux assay and the 30-fold difference in blocking affinity for the rat muscle K(Ca) channel could reflect a similar discrimination of K^+ channel subtypes. Although application of charybdotoxin peptides to problems in K^+ channel research is at an early stage, their potential usefulness remains promising.

Limited availability is, however, a major drawback since ChTX peptides appear to comprise only about 0.2% of crude *Leiurus* venom. Purification from the natural source is accordingly expensive and provides only small quantities of pure toxin for biochemical applications. In this regard, the collected sequences and relative activities of homologs provide structure-activity information that may ultimately lead to development of synthetic charybdotoxins. In the interim, work with the natural peptides must take advantage of sensitive chemical and electrophysiological methods for analyzing peptide structure and biological activity.

We were able to purify a sufficient quantity of ChTX-Lq1 to independently confirm the sequence of Gimenez-Gallego et al. [12]. In the case of ChTX-Lq2, the low abundance of this peptide and the difficulty of separating it from ChTX-Lq1 was particularly acute. Impurity of our final ChTX-Lq2 sample was evident from its HPLC profile and a few discrepancies between sequence data and amino acid composition. Histogram analysis of the blocked dwell times of ChTX-Lq2 also showed that the sample contained a mixture of two active toxins. Since the single-channel assay is capable of resolving kinetic parameters for mixtures of discrete blockers that have different dissociation rates, we utilized this system to characterize the activity of ChTX-Lq2 and iodinated derivatives of ChTX-Lq1.

Chemical contamination of a low affinity derivative with small amounts of a high affinity derivative can disguise the intrinsic activity of a low affinity compound that is being studied for quantitative structure-activity analysis. In traditional macroscopic assays of drug activity, it is usually impossible to address this problem other than to make exhaustive efforts at chemical purification. As an example, one can calculate that if a drug sample is contaminated with 5% of a competitive derivative that binds to a site with 10^3-fold higher affinity than the major low-affinity compound, then the observed equilibrium dissociation constant for the sample will be about 50-fold lower than the true value for the low-affinity compound. We first recognized the unique advantages of single-channel assays for such situations in structure-activity investigations of blocking of single sodium channels by saxitoxin derivatives [19]. In working with chemically-labile sulfated saxitoxin derivatives we observed that pure toxin samples could be reliably identified by monoexponential blocked time histograms, while old and degraded toxin samples exhibited multi-exponential distributions with blocked lifetimes characteristic of the various components. The histogram method presented and utilized in this paper provides a direct approach to the quantitative interpretation of such data.

Application of this method to the iodinated derivatives of ChTX-Lq1 shows that iodination impairs blocking activity by increasing the toxin's dissociation rate and lowering the association rate. Lower blocking affinity appears to result from both the iodination of a single tyrosine at position-36 and oxidation, possibly at the methionine-29. This interpretation of the iodination chemistry and the high conservation of the C-terminal region of the ChTX family (Fig. 3) suggests that this portion of the peptide is important in binding interactions with the K(Ca) channel and/or for native structure of the toxin. Inhibition of protein activity by tyrosine iodination has been commonly observed for other peptides and enzymes [26] and is considered to be due to the large size of the iodine atom (similar to the diameter of a benzene ring) and lowering of the pK_a of the tyrosine hydroxyl group which could perturb electrostatic interactions in its vicinity.

The large inhibitory effect (40 to 100-fold) of iodination on the observed association rate constant of ChTX-Lq1 is noteworthy. This severe lowering of the association rate constant is responsible for kinetic contamination of the blocked time histograms of our iodinated samples. Equations (3) and (4) show that even if a sample is 90% pure by concentration, a contaminant will contribute a significant proportion of blocking events if its association rate is higher than the major chemical component. Even though the new ChTX derivatives described in this paper are low affinity, they are instructive of the dependence of peptide binding rates on structure, whether by residue substitution in the case of ChTX-Lq2 or by iodination of a single residue. Our results also serve as a warning of possible misinterpretation of experiments on toxin derivatization unless careful attention is paid to the kinetic homogeneity of blocking activity.

A peptide ligand with the binding parameters of ^{125}I-Lq1a is unlikely to be useful in binding experiments aimed at identifying a toxin acceptor site corresponding to the large conductance K(Ca) channel in various tissues. However, since the affinity of Lq1 can be increased by about fourfold by lowering temperature [3] and replacement of KCl for NaCl in the internal medium [16], it is possible that specific binding of ^{125}I-Lq1a might still be detectable under these conditions. Also, since ChTX has been shown to be a potent inhibitor of other types of voltage-activated K^+ channels [6, 14, 17], it is possible that toxin binding to these other K^+ channel subtypes may not be as sensitive to iodination as the K(Ca) channel from skeletal muscle. In order to explore this possibility, we measured direct binding of ^{125}I-Lq1a to rat muscle membranes at 0°C and at low ionic strength (50 mM NaCl) using standard binding filtration techniques. In such experiments, we did observe binding of ^{125}I-Lq1a that could be displaced by native ChTX-Lq1, but this binding was low affinity (K_d > 200 nM). Since displacement titrations also showed a low affinity for native ChTX-Lq1, it appears that this binding is not due to the K(Ca) channel as studied in bilayers (K. Lucchesi, *unpublished results*). Further experiments are required to determine whether such low affinity binding is "nonspecific" or due to another potassium channel subtype in skeletal muscle. Using methods similar to those described in this paper, other types of chemically labeled ChTX-derivatives can be screened for K(Ca) channel blocking activity in search of an appropriate ligand for biochemical applications.

Dedicated technical assistance in toxin purification was provided by John Specht, Rosemary Keffer and Richard Syzpula. Drs. Deborah Lieberman and Kenneth Blumenthal at the University of Cincinnati and Robert Dreyer at Yale collaborated in HPLC purification of ChTX peptides in the early phase of this work. Amino acid analysis and microsequencing was performed in collaboration with Ms. Kathy Stone and Dr. Ken Williams of the Yale Peptide Chemistry Facility. We especially thank Dr. Chris Miller and members of his laboratory at Brandeis for consultation and manuscripts of unpublished work.

This work was supported by NIH grants HL38156, AR38796 and a grant from the Searle Scholars Program/Chicago Community Trust. E.M. is supported by an Established Investigator award from the American Heart Association.

References

1. Abia, A., Lobaton, C.D., Moreno, A., Garcia-Sancho, J. 1986. *Leiurus quinquestriatus* venom inhibits different kinds of Ca^{2+}-dependent K^+ channels. *Biochim. Biophys. Acta* **856**:403–407
2. Allen, G. 1981. Sequencing of Proteins and Peptides. Elsevier, New York
3. Anderson, C.S. 1987. The Interaction of Charybdotoxin with the Calcium-Activated Potassium Channel from Mammalian Skeletal Muscle. Ph.D. thesis. Graduate Department of Biochemistry, Brandeis University, Waltham
4. Anderson, C.S., MacKinnon, R., Smith, C., Miller, C. 1988. Charybdotoxin block of single Ca^{2+}-activated K^+ channels: Effects of channel gating, voltage and ionic strength. *J. Gen. Physiol.* **91**:335–349
5. Burgess, G.M., Claret, M., Jenkinson, D.H. 1981. Effects of quinine and apamin on the calcium-dependent potassium permeability of mammalian hepatocytes and red cells. *J. Physiol. (London)* **317**:67–90
6. Cahalan, M.D., Lewis, R.S. 1988. Role of potassium and chloride channels in volume regulation by T lymphocytes. *In:* Cell Physiology of Blood. R.B. Gunn and J.C. Parker, editors. pp. 281–301. Rockefeller University Press, New York
7. Carbone, E., Wanke, E., Prestipino, G., Possani, L.D., Maelicke, A. 1982. Selective blockage of voltage-dependent

K^+ channels by a novel scorpion toxin. *Nature (London)* **296:**90–91
8. Castle, N.A., Strong, P.N. 1986. Identification of two toxins from scorpion (*Leiurus quinquestriatus*) venom which block distinct classes of calcium-activated potassium channel. *FEBS Lett.* **209:**117–121
9. Catterall, W.A. 1977. Membrane potential-dependent binding of scorpion toxin to the action potential Na^+ ionophore: Studies with a toxin derivative prepared by lactoperoxidase-catalyzed iodination. *J. Biol. Chem.* **252:**8660–8668
10. Catterall, W.A., Morrow, C.S., Daly, J.W., Brown, G.B. 1981. Binding of batrachotoxinin A 20-α-benzoate to a receptor site associated with sodium channels in synaptic nerve ending particles. *J. Biol. Chem.* **256:**8922–8927
11. Cook, N.S. 1988. The pharmacology of potassium channels and their therapeutic potential. *Trends Pharmacol. Sci.* **9:**21–28
12. Gimenez-Gallego, G., Navia, M.A., Reuben, J.P., Katz, G.M., Kaczorowski, G.J., Garcia, M.L. 1988. Purification, sequence and model structure of charybdotoxin, a potent selective inhibitor of calcium-activated potassium channels. *Proc. Natl. Acad. Sci. USA* **85:**3329–3333
13. Harvey, A.L., Anderson, A.J. 1985. Dendrotoxins: Snake toxins that block potassium channels and facilitate neurotransmitter release. *Pharmac. Ther.* **31:**33–55
14. Lewis, R.S., Cahalan, M.D. 1988. Subset-specific expression of potassium channels in developing murine T-lymphocytes. *Science* **239:**771–775
15. Lucchesi, K.J., Moczydlowski, E. 1989. Block of K(Ca) channels by mono-iodinated charybdotoxin derivatives and a newly identified homolog. *Biophys. J.* **55:**547*a*
16. MacKinnon, R., Miller, C. 1988. Mechanism of charybdotoxin block of the high-conductance Ca^{2+}-activated K^+ channel. *J. Gen. Physiol.* **91:**335–349
17. MacKinnon, R., Reinhart, P.H., White, M.M. 1988. Charybdotoxin block of *shaker* K^+ channels suggests that different types of K^+ channels share common structural features. *Neuron* **1:**997–1001
18. Miller, C., Moczydlowski, E., Latorre, R., Phillips, M. 1985. Charybdotoxin, a protein inhibitor of single Ca^{2+}-activated K^+ channels from mammalian skeletal muscle. *Nature (London)* **313:**316–318
19. Moczydlowski, E., Hall, S., Garber, S.S., Strichartz, G.R., Miller, C. 1984. Voltage-dependent blockade of muscle Na^+ channels by guanidinium toxins: Effect of toxin charge. *J. Gen. Physiol.* **84:**687–704
20. Moczydlowski, E., Latorre, R. 1983. Gating kinetics of Ca^{2+}-activated K^+ channels from rat muscle incorporated into planar lipid bilayers: Evidence for two voltage-dependent Ca^{2+} binding reactions. *J. Gen. Physiol.* **82:**511–542
21. Moczydlowski, E., Lucchesi, K., Ravindran, A. 1989. An emerging pharmacology of peptide toxins targeted against potassium channels. *J. Membrane Biol.* **105:**95–111
22. Olivera, B.M., Gray, W.R., Zeikus, R., McIntosh, J.M., Varga, J., Rivier, J., deSantos, V., Cruz, L.J. 1985. Peptide neurotoxins from fish-hunting cone snails. *Science* **230:**1338–1343
23. Podell, D.N., Abraham, G.N. 1978. A technique for the removal of pyroglutamic acid from the amino terminus of proteins using calf liver pyroglutamate amino peptidase. *Biochem. Biophys. Res. Commun.* **81:**176–185
24. Possani, L.D., Martin, B.M., Svendsen, I. 1982. The primary structure of noxiustoxin: a K^+ channel blocking peptide, purified from the venom of the scorpion *Centruroides noxius* Hoffmann. *Carlsberg Res. Commun.* **47:**285–289
25. Ravindran, A., Moczydlowski, E. 1989. Influence of negative surface charge on toxin binding to canine heart Na channels in planar bilayer. *Biophys. J.* **55:**359–365
26. Regoeczi, E. 1984. Iodine-Labeled Plasma Proteins. CRC, Boca Raton, FL
27. Sigworth, F.J., Sine, S.M. 1987. Data transformation for improved display and fitting of single-channel dwell time histograms. *Biophys. J.* **52:**1047–1054
28. Smith, C., Phillips, M., Miller, C. 1986. Purification of charybdotoxin, a specific inhibitor of the high-conductance Ca^{2+}-activated K^- channel. *J. Biol. Chem.* **261:**14607–14613
29. Valdivia, H.H., Smith, J.S., Martin, B.M., Coronado, R., Possani, L.D. 1988. Charybdotoxin and noxiustoxin, two homologous peptide inhibitors of the $K^+(Ca^{2+})$ channel. *FEBS Lett.* **226:**280–284
30. Watt, D.D., Simard, J.M. 1984. Neurotoxic proteins in scorpion venom. *J. Toxicol-Toxin Rev.* **3:**181–221
31. Wolff, D., Cecchi, X., Spalvins, A., Canessa, M. 1988. Charybdotoxin blocks with high affinity the Ca-activated K^+ channel of Hb A and Hb S red cells: Individual differences in the number of channels. *J. Membrane Biol.* **106:**243–252

Received 7 February 1989